Molecular Simulation, Vol. 31, No. 14–15, 15–30 December 2005, 1005–1017

Taylor & Francis
Taylor & Francis Group

Standards for molecular dynamics modelling and simulation of relaxation

A. Y. KUKSIN, I. V. MOROZOV*, G. E. NORMAN, V. V. STEGAILOV and I. A. VALUEV

Institute for High Energy Densities, Russian Academy of Sciences, Izhorskaya Street 13/19, Moscow 125412, Russia

(Received October 2005; in final form October 2005)

An attempt is made to formulate a set of requirements for simulation and modelling of relaxation in dense media. Each requirement is illustrated by examples of numerical simulation of particles with different types of interaction given by soft-sphere, Lennard–Jones, embedded atom method or Coulomb potential. The approaches developed are expected to be universal for some classes of relaxation processes in liquids, fluids, crystals and plasmas.

Keywords: Modelling of relaxation; Numerical simulation; Lennard–Jones potential; Coulomb potential; Molecular dynamics; Metastable states; Dynamical memory time

1. Introduction

Molecular dynamics (MD) modelling and simulation is one of the most important and effective methods in the modern computational physics of classical dense media. However, most of the papers where MD method is involved are devoted to the studying of equilibrium systems [1–6]. At the same time one might expect that MD method could be a powerful tool for studying non-equilibrium states and relaxation phenomena in dense many-particle systems. In this connection, we would mention studies of relaxation to equilibrium in two-component two-temperature non-ideal plasmas [7–11], damping oscillation regime in one-component non-ideal plasmas [12], recombination relaxation in ultracold plasmas [13–15], melting front velocity [16], spontaneous decay of a superheated or stretched crystal [17–20], relaxation of SH radical in solid krypton [21], protein folding [22], relaxation in shock wave front [23–26].

Any conventional equilibrium MD simulation starts from more or less arbitrary initial conditions. Then different approaches are applied to equilibrate the system. Only subsequent equilibrium runs are used to obtain useful information. The objective of the simulation of relaxation is of the opposite sense, i.e. to get the information from the non-equilibrium part of the MD run, from that part which is discarded and is not used in equilibrium MD simulations. It is evident that the requirements for the simulation and modelling of the relaxation should differ from those for the equilibrium ones.

Modelling and simulation of relaxation is a relatively new sector of computer physics where the standard of approaches, models and numerics has not yet been estblished. This paper contributes to the development of this standard. We use the experience which we gained from simulation of particular relaxation processes [8–11,17–20].

It should be noted that we deliberately use both terms: "simulation" and "modelling". Simulation means an implementation of a numerical scheme while modelling means choices of the initial and boundary conditions, definitions of the ensemble of initial non-equilibrium states, choices of the particle number, etc. Developing of procedures to measure relaxation related properties also belongs to modelling.

In order to emphasize the difference between equilibrium and non-equilibrium cases we start with the section where we present briefly the standard of MD modelling and simulation of equilibrium dense media. Then we proceed to the presentation and discussion of different items of the standard of MD modelling and simulation of relaxation: (a) the choice of the initial state and sampling of the ensemble of initial states; (b) the question of whether there are any features of the relaxation processes which are ensemble-independent; (c) the methods to analyse state of the system at a given moment of time; (d) the possibility of

*Corresponding author. Email: bogous@orc.ru

Molecular Simulation
ISSN 0892-7022 print/ISSN 1029-0435 online © 2005 Taylor & Francis
http://www.tandf.co.uk/journals
DOI: 10.1080/08927020500375259

measuring values, which need averaging over a relatively long period of time, for a non-stationary case. A relaxation process can be too long to be simulated by MD in particular for multi-scale systems; some recipes for such cases are given in the last section. All items of the standard are summarized in the conclusions.

To demonstrate both universal and particular features of the simulation and modelling, three examples of the relaxation in very dissimilar multi-scale systems are presented in this paper: (i) equilibration of electrons and ions in a non-isothermal non-ideal plasma; (ii) decay of metastable superheated crystals at both stationary heating and stationary temperature, their lifetime and subsequent nucleation processes; (iii) void formation in a crystal under negative pressures.

2. Modelling and simulation of equilibrium dense media

2.1 Equilibration

Initial conditions are chosen usually in the simplest way, for example random or crystal sites for initial positions of atoms. Then different approaches are applied to minimize the relaxation period and to achieve the equilibrium parameters needed. The fact that MD run proceeds to the stationary regime is checked by various criteria from the trivial, e.g. constance of average kinetic energy of particles, to more and more sophisticated, e.g. stationary behaviour of the root mean square displacement for equilibration and sampling of a biomolecule [27–32].

2.2 Boundary conditions and particle numbers

Boundary conditions should reflect the physical system to be studied: a uniform infinite volume, a surface, phase separations, clusters, etc.

The choice of particle number N is performed according to spatial and temporal requirements and restrictions.

The length of the simulation box edge L should be greater or much greater than the correlation length. Since there is a hierarchy of correlation lengths the choice of N restricts us to the study of a definite set of correlations. The same is valid for the restriction of the wave vector of fluctuations (plasma waves, phonons, etc.) for a given N. Another requirement is related to the contribution of interparticle interactions at distances outside the simulation box. This contribution should not be remarkable otherwise periodic boundary conditions are able to impose a correlation which in fact does not exist.

According to the temporal restrictions the squared length L^2 should be greater than the diffusion coefficient multiplied by the correlation time. Another restriction says that L/v_s, where v_s is the sound velocity, should be greater than the correlation time under study; the N-dependence in MD calculations of velocity autocorrelation functions is demonstrated in [33]. Since there is also a hierarchy of correlation times the choice of N restricts us to study a definite set of time correlations.

The requirements to N mentioned above are related to the simulation of uniform media. Apparent additional requirements appear for the MD simulation of surfaces, phase equilibria, etc.

2.3 Numerical integration

Numerical integration time step Δt should be much smaller than the inverse value of the maximum oscillation frequency in the system. Another physical restriction strongly limits Δt by the characteristic length of the remarkable variation of the potential energy divided by the particle thermal velocity. Other restrictions are of the computational character, cf. [34–36].

The duration of MD run $t_{\max}$ defines the accuracy of averaging which is not less than $\sim M^{-1/2}$, where $M = t_{\max}/t_m$ and t_m is a dynamic memory time [34–36] (see below). Averaging over particles if available increases accuracy by a factor $N^{-1/2}$. Grows of N reduces the performance by a factor of N^2 (or at least $N \log N$) for long-range potentials and by a factor of N for short-range potentials being less effective than averaging over an ensemble.

3. Modification of equilibrium requirements for non-stationary case

All the above mentioned items are to be substituted or at least supplemented and modified to study relaxation phenomena. Consider first the requirements which can be modified.

The requirements to the boundary condition are of the same character. Additional difficulties appear when non-stationary boundary conditions are needed, e.g. at the simulation of shock wave propagation [23–26], etc.

Correlation lengths do not remain constant during the relaxation. Account of these lengths is important when cooperative phenomena are considered, e.g. nucleation or plasma waves. The MD box size should be greater than the maximum correlation length which might appear during the relaxation process. Appearance of a local non-equilibrium state in the small subsystem ($N \lesssim 10^3$ particles) of a uniform equilibrium system was observed in MD simulations [37].

Numerical integration with a variable time step is applied if the relaxation includes a dramatic increase of velocities of some particles [14]. Pair distribution function could be a sensitive tool to detect particles which could approach potentially forbidden small distances due to insufficiently small time step.

The equilibration procedures used in conventional equilibrium MD simulations are more or less artificial. Their main objective is to achieve equilibrium by any means as fast as possible. Therefore these procedures make no sense to study real relaxation processes. The averaging procedure should be substituted by another one as well. The new requirements for equilibration, averaging and diagnostics are considered in the subsequent sections.

4. Initial state: ensemble of initial states

The choice of the initial state cannot be an arbitrary one as it should correspond to the physical problem we would like to study. The physical system is modelled with respect to the boundary conditions, particular non-equilibrium conditions and the minimum particle number which is required to reproduce the main features of the relaxation process studied.

One initial state is not sufficient as a rule to achieve the satisfactory accuracy. So an ensemble of initial states is needed to obtain a number of MD runs and perform the averaging of the results. Each microscopic state in the ensemble should differ from each other significantly but all of them are to be equivalent with respect to the macroscopic non-equilibrium state under study. The last requirement needs some art and can be checked by the following criteria. The increase of the number I of initial states increases the accuracy of averaging as $\sqrt{I}$ and does not shift the mean value.

4.1 Non-equilibrium plasmas

Let us consider several examples of modelling of initial states of non-equilibrium strongly coupled (non-ideal) plasmas.

The first example is modelling of relaxation in non-ideal plasmas created after ultrafast laser heating, e.g. by a femtosecond pulse. The following initial conditions can be suggested for this case:

- ion coordinates are taken to be random for a gaseous target, or crystal-like for a solid target;
- ion velocities are taken to be Maxwellian for initial temperature of the target, e.g. 300K, or ion velocities can be assumed to be zero in the case of a very strong laser field;
- electron coordinates are taken to be random in the vicinity of ions;
- the absolute values of electron velocities satisfy the equation of energy conservation $U + (m_e v^2/2) = n\hbar\omega - I$, where v is the electron velocity, $n\hbar\omega$ is absorbed energy, I is the ionization potential, U is the potential energy of particle interaction.

The random choice of the particle coordinates and velocity directions gives us a perfect opportunity to generate an ensemble of equivalent but different initial state.

The initial positions of electrons can be assigned randomly or taken from an equilibrium MD run. In the first case one should apply a Monte–Carlo procedure to achieve given value of U. In the second case the average value of U is guaranteed to be the same as in the equilibrium trajectory.

Another example is a relaxation in a shock-compressed plasma. To get the initial distributions of ion velocities and coordinates it is necessary to simulate a smooth front formation according to [23–26]. Possible initial conditions implies zero velocities of electrons.

Some simplified initial conditions are used in [9–11]. The initial state for the coordinates of the particles are taken from corresponding equilibrium simulations. The velocities are to be changed according to the physical case modelled.

Non-equilibrium plasma created by an instantaneous change of Debye radius is considered in [38].

4.2 Metastable states

Deploying MD technique one can investigate metastable states that are relatively close to the boundary of stability of the given phase. Their lifetimes are short enough to be within the computational capabilities.

One MD run gives us a value of the particular lifetime for a given initial configuration in the phase space. Then averaging should be performed over the ensemble of initial configurations. To prepare such an ensemble of microscopic configurations we should fix the macroscopic conditions that determine the degree of metastability, e.g. the values of temperature and density in the case of superheating/undercooling. Then MD trajectories calculated from each of the initial conditions of the ensemble give us the set of the lifetime values. Average over lifetimes results in a mean value $\bar{\tau}$ which is specific for the given degree of metastability and the volume studied.

For example, there are several ways to obtain the ensemble of microscopic configurations that correspond to the superheated crystal. One can start from a crystal at temperature below the melting temperature heating it up to the desired temperature. To prevent lattice disordering the artificial constraints on the particle motion are applied. The particles are bounded inside a sphere or the Wigner–Zeitz cell with reflective walls. A quasi-equilibrium MD trajectory can be calculated with these constraints. Then an ensemble of M independent phase points can be taken from this trajectory as an initial states for M runs without restrictions on particle motion. Each run provides a lifetime as shown in figure 1.

The set of lifetime values can form a certain type distribution, e.g. an exponential distribution if the metastable phase decay goes as a Poisson random process (figure 2).

4.3 Parallel computations

In general, MD code is hard to parallelize because of many network communications required for the force calculation procedure. An alternative parallelizing algorithm is possible in case of simulation of the relaxation. Since averaging over initial states is required, the relaxation from different initial states can be calculated in parallel. The network load is very low in this case. Therefore the parallel algorithm should be used to calculate the relaxation whereas the standard one is used to obtain an ensemble of initial states.

The general idea of the parallel essence of MD simulations of relaxation is illustrated in figure 3. The durations of parallel relaxation MD runs in Set II can be equal to each other, as in simulations of plasma relaxation, or not equal to each other, as in the case of calculation of metastable state lifetime distribution. An alternative parallel procedure of the generating of the ensemble of relaxation MD runs is discussed in the next section. However, it is more restricted in applications.

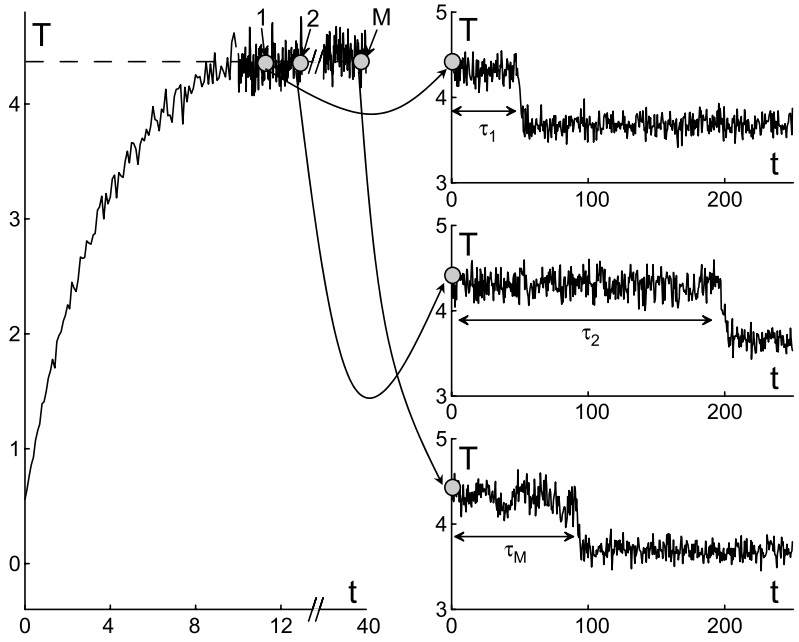

Figure 1. Left side of the plot: the temperature dependence on time during heating to the desired temperature when the restrictions on particle motion are applied. Right side: three examples of MD runs without restrictions. Each of them gives the value of lifetime $\tau_j, j = 1, 2, \ldots M$. (Results were obtained for the Lennard–Jones system, $N = 500$ particles, density $1.2\sigma^{-3}$).

5. Ensemble-dependence

Non-equilibrium states can differ for different ways of excitation of the same media. Each non-equilibrium state corresponds to a certain ensemble of initial states in simulations. The problem is to distinguish quantities which are ensemble-dependent, i.e. characterise both medium and the way of excitation, from those which characterise the medium and are independent of the way of excitation.

The inherent feature of MD systems is the Lyapunov instability. Due to this instability there appears a dynamic memory time t_m which limits time interval when the Caushy problem is valid for MD numerical integration. For times greater than t_m MD trajectory 'forgets' its initial conditions and ceases to correlate with the hypothetical Newtonian trajectory started from the same initial conditions [34–36]. We expect that the duration of ensemble-dependent part of the relaxation correlates with t_m.

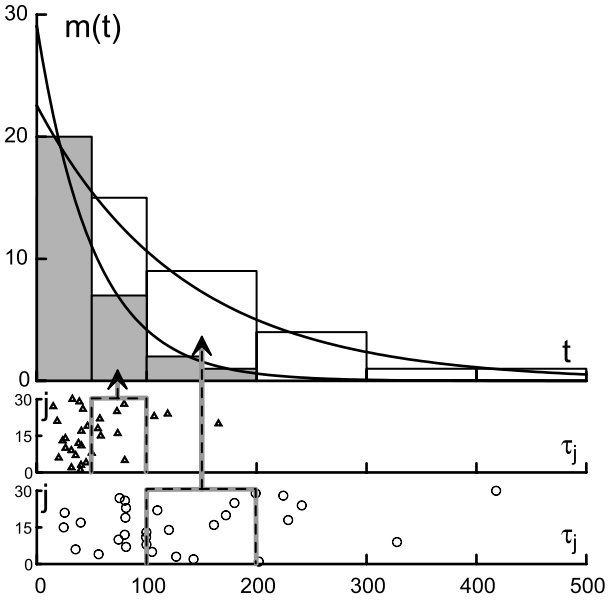

Figure 2. Distributions of lifetime values for two different temperatures, $m(t)$ is the number of MD runs, for which the superheated solid decay happened in the time interval $(t, t + \Delta t)$. The original lifetimes are given on two subplots: j is the number of the MD run in figure 1 and τ is the corresponding value of lifetime. Results were obtained for the Lennard–Jones system with $N = 6912$ particles, density equals to $1.0\sigma^{-3}$, $M = 30$ MD runs, temperatures $T = 1.6097$ (grey distribution), $T = 1.5871$ (white distribution). Solid lines correspond to $m(t) = (M\Delta t/(\bar{\tau}^2)\exp(-t/\bar{\tau})$, where Δt is the width of histogram bars.

5.1 Electron–ion relaxation

Ensemble-dependence can be illustrated by the results of MD simulation of the non-ideal plasma. Such plasma is usually characterised by a non-ideality (coupling) parameter $\Gamma = e^2(4\pi n_e/3)^{1/3}/(k_B T)$ or the Debye number $N_D = (kT)^{3/2}/(3e^2\sqrt{\sqrt{4\pi n_e}})$, where T is the final temperature at

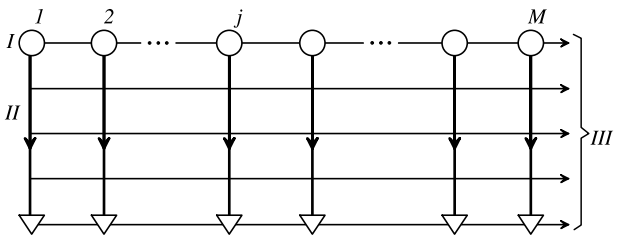

Figure 3. Schematic picture of the inherent parallelism of MD simulations of relaxation: I—a set of initial conditions (circles), generated by a certain procedure (MD run, set of random phase space coordinates, etc.); II—a set of independent relaxation MD runs, which should be average by a procedure III. Triangles are the final points.

the end of relaxation, n_e is the number density of electrons. Let us consider a fully-ionized two-component plasma of N electrons and N singly ionized ions with masses m and M, respectively. The particles exert each other with a quasi-classical interaction potential such as 'corrected Kelbg' pseudopotential [39]. The number of ions in those particular simulations is $N = 64-800$. Choice of N and N-independence are discussed elsewhere [9,10].

The initial non-equilibrium state is characterised by different temperatures of electrons T_e and ions T_i. We used the initial conditions where the velocities of electrons or/and ions are equal to zero (see previous section for details). The results of MD runs are averaged over an ensemble of $I = 50-200$ initial states. Provided the result is N-independent, the relative error is given by $1/\sqrt{NI}$ which agrees with direct calculation of normal statistical deviation shown in plots by error bars. Exactly these error bars correspond to the confidence coefficient 0.68. They are not plotted if they are smaller than the size of the points.

As seen from figure 4 the relaxation is characterised by initial oscillations at the first stage and by the subsequent decrease of the difference between electron and ion temperatures $\Delta T = |T_e - T_i|$ where the values of T_e and T_i are the average kinetic energy of the particles $T(t) = \frac{1}{2NI}\sum_{j,k}^{N,I} m v_{jk}^2(t)$. The time here and below is measured in units of the period of electron plasma oscillations $\tau_e = 2\pi/\omega_p$, $\omega_p = \sqrt{4\pi n_e e^2/m}$.

It follows from the Boltzmann equation that $\Delta T \sim \exp\{-t/\tau_B\}$. This result is based on the assumption that the collisions between the particles are statistically independent. Therefore, it can describe only the stochastic part of relaxation which does not depend on the initial ensemble.

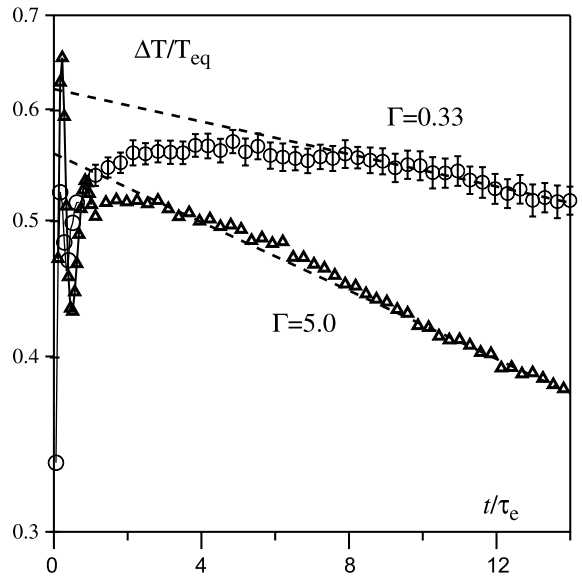

Figure 4. Difference between mean kinetic energies of electrons and ions $\Delta T = |T_e - T_i|$ depending on time. Initial conditions: $T_e(0) = T_i(0) = 0$. The value of ΔT is normalized by the equilibrium temperature $T_{equation}$ In order to define τ_{nB} and the beginning of exponential decay the long time scale relaxation is fitted by the dash straight line. $M/m = 100$.

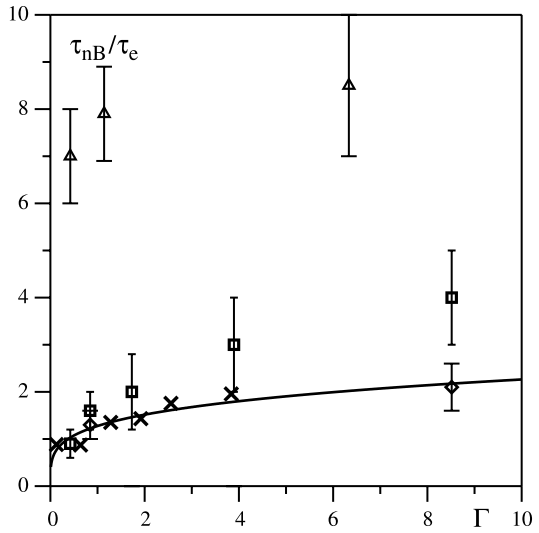

Figure 5. Dependence of the duration of the non-exponential relaxation stage τ_{nB} on the non-ideality parameter for different initial conditions: $T_i(0) = 0$—squares, $T_e(0) = 0$—rhombus, $T_e(0) = T_i(0) = 0$—triangles. The dynamical memory time t_m—crosses, the solid line is the power fit $t_m \sim \Gamma^{0.25}$.

For a non-ideal plasma the exponential relaxation derived from the Boltzmann equation is obtained only for an asymptotic behaviour. The duration of the non-exponential relaxation stage τ_{nB} which precedes the exponential one is shown on figure 5 depending on the non-ideality parameter. The value of τ_{nB} is almost independent of the mass ratio provided that $M/m \geq 100$ [11]. As seen from figure 5 the value of τ_{nB} depends on the initial conditions within the order of magnitude but stays comparable with t_m. This implies that the non-exponential stage corresponds to the dynamic relaxation while the exponential one corresponds to the stochastic relaxation in agreement with statements underlying the Boltzmann theory. In such a strongly correlated plasma the time of the stochastization t_m becomes greater than the time between collisions [34] and the role of non-exponential relaxation becomes significant.

5.2 Decay of a metastable phase

As already mentioned a set of lifetime values can be obtained for the ensemble of the microscopic initial configurations corresponding to the given macroscopic condition of the metastable state.

Provided that $\bar{\tau} > t_m$, MD runs with different integration time steps even for the same initial configuration will result in a set of different lifetimes [17,19]. Apparently after the initial time t_m the system 'forgets' its initial condition and trajectories calculated with different time steps become statistically independent. Since the value of the dynamical memory time grows only logarithmically as the accuracy of integration increases, it is practically impossible to calculate the exact dynamic value of lifetime for the given initial configuration if $\tau > t_m$.

Using this fact one can estimate the value of the average lifetime from calculations with different integration time steps (figure 6). Such distributions are close to those obtained

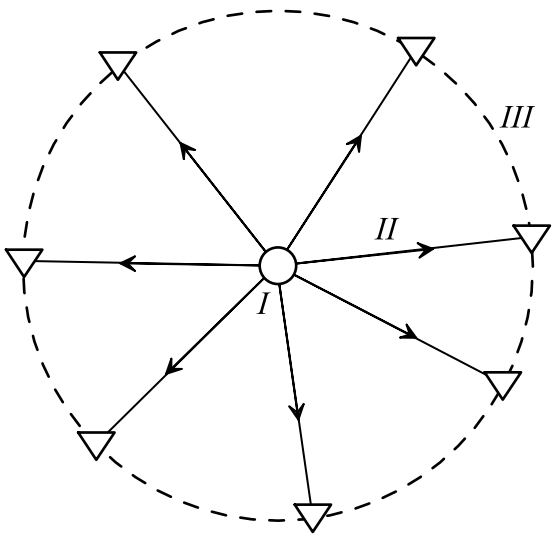

Figure 6. Schematic picture of the inherent parallelism of MD simulation of relaxation, following from the Lyapunov divergency of MD trajectories. The set II and procedure III are the same as in figure 3, the set I is reduced to only one point.

for the ensemble of different initial configurations discussed above in figures 1–3.

6. Instantaneous diagnostics

New procedures are to be developed to find characteristics of relaxation at a given moment of time, e.g. to find parameters which qualitatively show the overall degree of deviation from the Maxwellian velocity distribution and from the Gaussian distribution of crystal particles in space. More details about these deviations can be found from calculation of the distributions themselves. This diagnostic can be applied separately to different spatial regions in non-homogeneous case.

6.1 Non-ideal plasma

First let us consider relaxation of velocity distribution functions in a non-ideal plasma. It is suitable to choose initial conditions like $T_e(0) = T_i(0) = 0$ to observe all stages of relaxation [9]. Heating of charges in this case is provided by the decrease of the potential energy (disorder induced heating). The velocity distribution functions for both electrons and ions are presented in figure 7. At the first presented time moment neither electrons nor ions have the equilibrium distribution. Then at $t \backsimeq 0.6\tau_e$ the Maxwell distribution is built up for electrons while ions are in the non-equilibrium state. Finally, one will have two equilibrium distributions with different temperatures at $t \backsimeq 15\tau_e$, which then relax to the total equilibrium with equal temperatures. All these plots were obtained by averaging results picked up from different MD runs which correspond to one ensemble of initial states.

Notice that the difference between average energies of electrons and ions proceeds to the exponential decay after $t \backsimeq 6\tau_e$, i.e. earlier than the Maxwell distribution is built up for ions. The equilibrium between potential and kinetic particle energies of electrons and ions is achieved at $T \backsimeq 100\tau_e$ for the case considered [9].

6.2 Decay of a metastable crystal at stationary temperature

A condensed matter can exist at negative pressures. Such states were observed experimentally, e.g. in [40]. States under negative pressure are metastable ones, so they can exist for only a limited period of time. They decay spontaneously after that and result in formation of voids.

A system under study is a f.c.c. crystal of particles interacting via Lennard–Jones potential $U(r) = 4\epsilon((\sigma/r)^{12} - (\sigma/r)^6)$. Periodic boundary conditions are used. The values of temperature T and number density ρ are chosen for the simulation to obtain a state near the spinodal in order its lifetime can be reached during the MD run. Initial velocities are taken from the Maxwellian distribution.

The results of a certain example are presented in figure 8 for time dependencies for T, pressure P and Lindemann parameter $\delta_L = \langle \Delta r^2 \rangle / r_{nn}$, where $\langle \Delta r^2 \rangle$ is the displacement of particles from the f.c.c. lattice sites averaged over all the particles in the simulation box at the current time step, r_{nn}

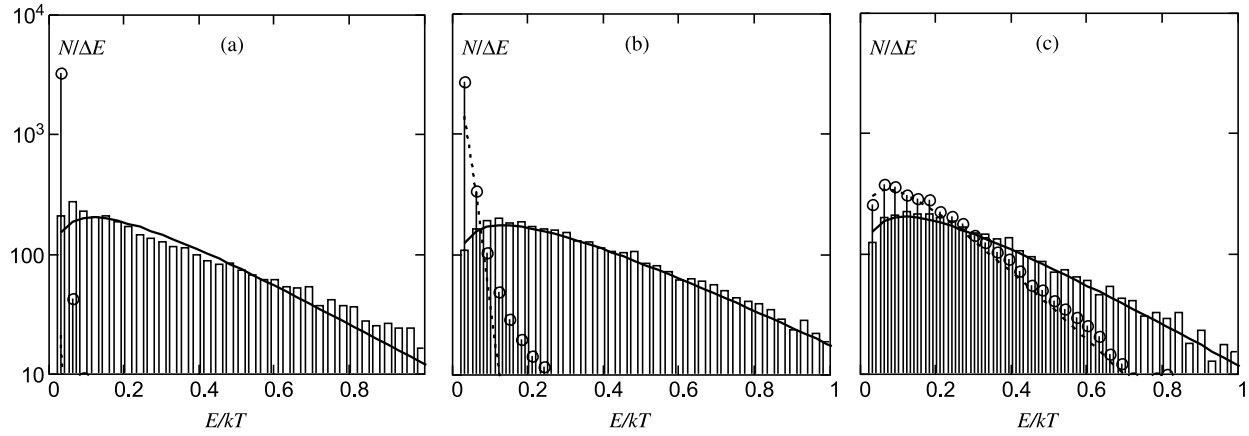

Figure 7. The energy spectra for electrons (bars) and ions (circles) at three moments of time corresponding to different stages of relaxation: (a) $t = 0.15\ \tau_e$; (b) $t = 0.58\ \tau_e$; (c) $t = 15\ \tau_e$. Solid and dashed line corresponds to the Maxwell distribution for electrons and ions calculated using the mean kinetic energy. $T_e(0) = T_i(0) = 0$, $\Gamma = 3.3$, $M/m = 100$.

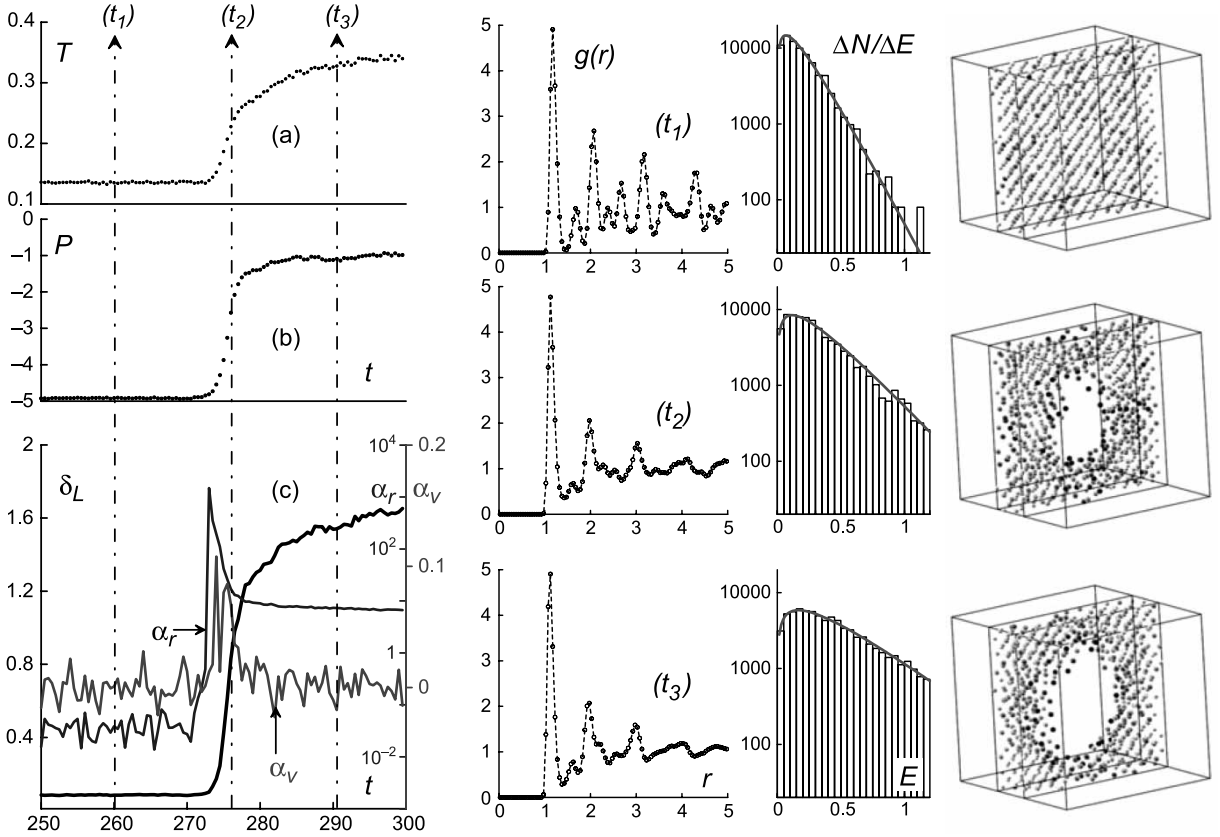

Figure 8. The combined plot describing kinetics of the stretched solid spontaneous decay ($\rho\sigma^3 = 1$, $N = 4000$, LJ units): (*a*) and (*b*)—temperature T and pressure P dependencies on time t; (*c*)—time dependencies for Lindemann parameter δ_L, non-Gaussian parameters of particle displacements α_r and velocities α_v. Radial distribution functions $g(r)$, kinetic energy distributions $\Delta N(E)/\Delta E$ (compared with the Maxwellian distributions for the relevant temperature) and particle structure cross-sections are presented for the three subsequent time moments.

is the nearest neighbor distance in the perfect lattice. Parameters $\alpha_r = (3/5)(\langle\Delta r^4\rangle/\langle\Delta r^2\rangle^2) - 1$ and $\alpha_v = (3/5)(\langle\Delta v^4\rangle/\langle\Delta v^2\rangle^2) - 1$ show the degree of deviation from the Gaussian distribution for particle displacements and velocities respectively, $\alpha_r = \alpha_v = 0$ for the Gaussian–Maxwellian distribution). The metastable state with stationary T and P exists during $\sim 275(m\sigma^2/\varepsilon)^{1/2}$ which is much greater than t_m, then spontaneous decay starts. It takes only few time units to form new more or less stationary state. The non-zero value of α_v points to the fact that the Maxwellian distribution is broken during the short decay period.

The pair radial distribution function, kinetic energy distributions and particle structure cross-sections are presented for the three time moments denoted by arrows. The time t_1 corresponds to the long-range order structure. The structures at t_2 and t_3 reveal only short-range order.

The microscopic picture of the spontaneous decay is presented in figure 9 for a larger simulation cell. It is evident that the decay starts with the local disordering of the crystal structure. The voids appear in the melted regions only at the next stage of the decay. Another characteristic feature of the decay is observed: the structure formed is strongly non-uniform. At least three phase states can be distinguished: crystal clusters, disordered regions and voids. In fact the final state of our MD run is not an equilibrium one, since the pressure remains to be negative till the end of our simulation.

6.3 Decay a metastable crystal at stationary heating

Superheated solid is a state of matter that can be realized experimentally only under particular conditions of high rate energy impacts and/or very low concentration of defects and impurities which enables heterogeneous melting (see, e.g. [41]).

Simulations starts from an initially ideal crystal lattice. After 10^4 time steps the system is brought to the equilibrium at the temperature below the melting temperature. Then the model crystal undergoes isochoric heating at the constant rate $\dot{T} = 6 \times 10^{-4}(\epsilon^3/m\sigma^2)^{1/2}$. The heating is performed by velocity rescaling in the spirit of the Berendsen thermostat technique. As heating is being done (figure 10) the temperature of the model crystal becomes higher than the melting temperature for the given density $T_m = 1.25\epsilon$. When temperature reaches $T = 1.52\epsilon$ the crystal structure decays into fluid. Phase transformation leads to a rapid change of the averaged potential energy U.

Structural transformations manifest themselves through the changes of α_r and δ_L. According to the Lindemann criterion of melting δ_l equals to 0.12–0.13 for simple

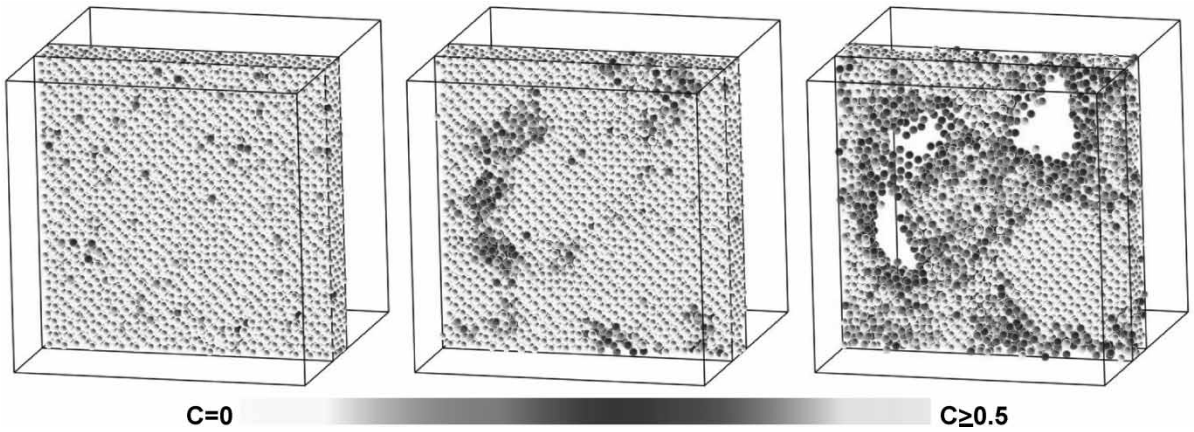

Figure 9. The microscopic picture of the slab inside the MD cell for three moments of time corresponding to the initial crystal structure, start of the decay process and final non-uniform structure. The colour of particles shows the degree of disordering. $N = 32{,}000$, $\rho = 0.8\sigma^{-3}$.

crystals at the melting temperature T_m. This relation holds for the case considered. However, at $T = T_m$ no phase transition appears but the crystal becomes superheated. The value of δ_l can achieve a value as high as 0.4 before the crystal decays. There is a peak on the α_r-dependence on time which might correspond to emergence of collective modes in the motion of particles. This phenomenon can be considered as a precursor of the decay under heating. It does not produce any effect on the dependence of potential energy on time, however, Lindemann parameter proceeds to a faster increase after this peak. After the decay the motion of particles becomes irregular, so that α_r vanishes and δ_L gets the diffusion-like dependence on time. The loss of long range order is well seen on the evolution of the radial distribution function and on the orthogonal projections of the particle structure in the simulation box.

The system evolution can be divided into three parts: (1) heating and superheating up to the appearance of the melting precursor; (2) emergence of collective modes in the particle motion; (3) decay to the fluid state. The process of the relaxation in the case of the superheated crystal decay is connected with homogeneous nucleation that allows to apply the formalism of the classical nucleation theory (see [17,18] for details).

7. Time-averaged diagnostics

Averaging over a relatively long period of time is also needed to obtain, e.g. the values of dynamic structure factor.

Usage of MD for obtaining physical properties of a stochastic system always imply averaging of the calculated properties over a representative set (usually more than 30) of independent system configurations. For the properties that are characterised by time, or correlations in time the averaging can be performed along the MD trajectory. Each two measurements of some physical property along the equilibrium trajectory which are separated in time by the interval greater than the correlation time of the system are considered statistically independent. The typical example of the important correlation property for a many-particle system is the dynamic structure factor (DSF), which is the space and time Fourier transform of density-density correlation function. DSF characterises the intensity of collective oscillations in the system at a certain frequency and wave vector. The measurement of DSF in the MD experiment requires long MD trajectories because the determination of DSF includes the positions of all particles during some period of time and no averaging over particles can be performed. Averaging over time along the MD trajectory is the most convenient way to obtain DSF. It is also the way most effective computationally, because Fast Fourier Transform procedure can be used to obtain the result in frequency space.

Averaging over time is a serious problem for non-equilibrium states, where the measured property can significantly change its value during the time evolution. We note that this is a technical problem connected with impossibility of averaging over long time, the property itself must have, however, its instantaneous value with defined physical meaning. To use time averaging in these situations the procedures are suggested [10,42] which imply freezing of the instantaneous non-equilibrium state for the period of measurement. The idea is to introduce the energy exchange with an external bath keeping constant the non-equilibrium excitation. It is necessary to check that this procedure does not transform the non-equilibrium state during the period of measurement. This external source is switched on temporarily, and if further evolution of the system needs to be investigated, it is switched off and the relaxation continues as if there were no period of freezing. Below we illustrate the freezing technique using the example of DSF study of beam-excited non-equilibrium electron–ion plasma. A permanently developing non-equilibrium is caused by an electron beam propagating through the plasma with constant velocity. This type of non-equilibrium states exists in some experiments when large electron flows arise in plasma. The aim of this simulation is to detect the excitation of non-equilibrium collective plasma oscillations which are permanently present in the case of beam-excited plasma.

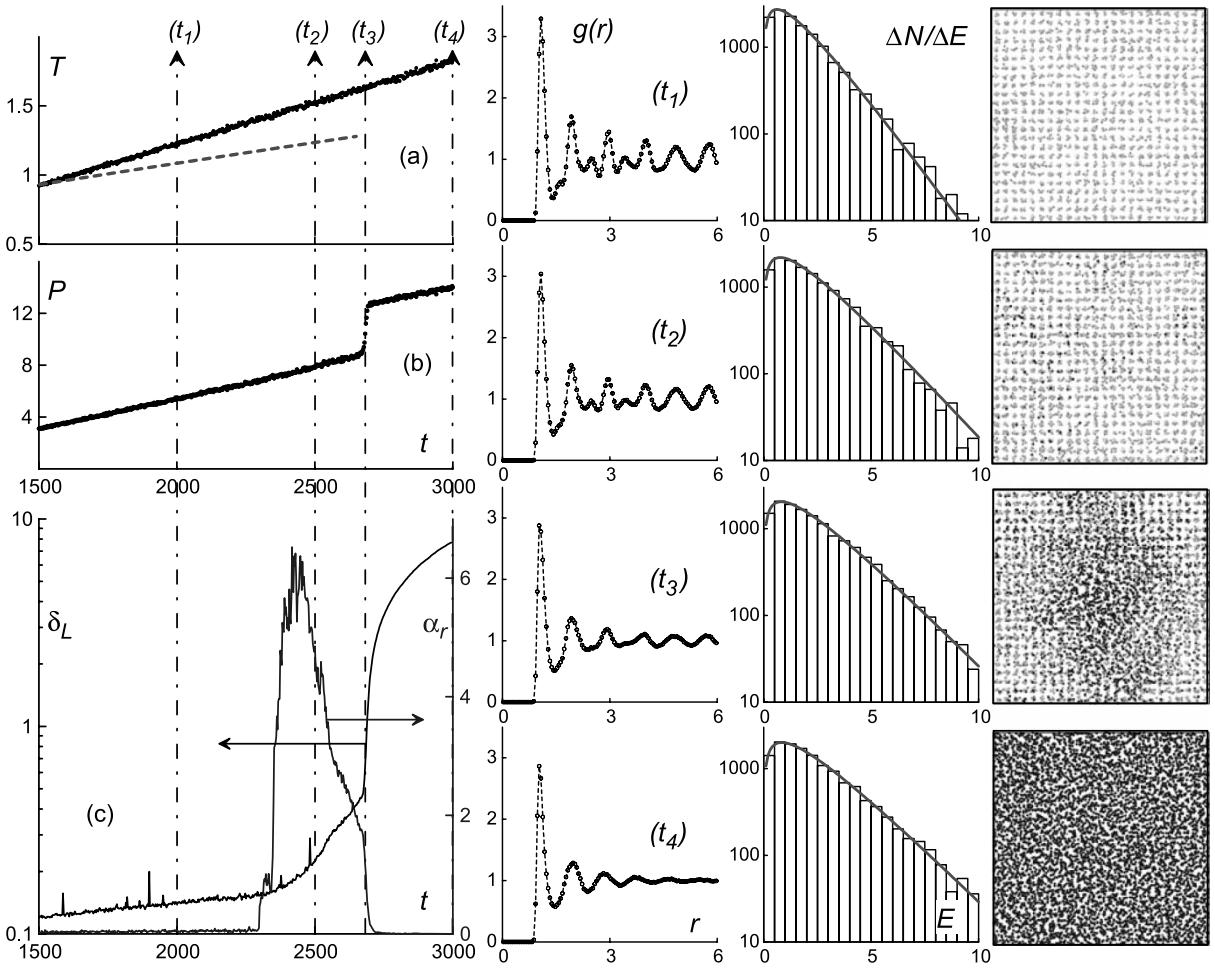

Figure 10. The combined plot describing kinetics of the crystal decay under constant rate heating $\dot{T} = 6 \times 10^{-4}(\epsilon^3/m\sigma^2)^{1/2}$ ($\rho\sigma^3 = 1, N = 6912$, LJ units): (*a*) and (*b*)—current temperature T and pressure P dependencies on time t (dashed line correspond to the equilibrium melting temperature at the current pressure $T_m(P)$); (*c*)—time dependencies for Lindemann parameter δ_L and non-Gaussian parameter of particle displacements α_r. Radial distribution functions $g(r)$, kinetic energy distributions $\Delta N(E)/\Delta E$ (compared with the Maxwellian distributions for the relevant temperature) and orthogonal projections of particle structure in the MD cell are presented for four subsequent time moments.

For the MD simulation a model of Hydrogen plasma (with realistic electron to ion mass ratio) consisting of 400 particles placed in the cell with periodic boundary conditions is used. The number of particle chosen is sufficient to study oscillations at plasma frequencies [11], and this choice does not influence very much the results of all simulations presented below. Interaction between electrons and ions is described by the pair Coulomb potential modified at small separations [8,11,39] to exclude for quantum bound states. Particles of the same type interact via the bare Coulomb potential. Equilibrium state prepared by Monte–Carlo procedure is used as initial condition for the MD experiment. The initial equilibrium parameters for the plasma are $\Gamma = 1$, $T = 30{,}000$K.

After preparing the system in equilibrium state with desired parameters, a number of extra electrons simulating the beam is driven through the system in one direction with constant velocity vector. The trajectories of these extra electrons are randomly selected for each extra electron entering the simulation cell and reselected when it crosses the cell boundary. Extra electrons interact with plasma particles, but their own velocities and trajectories are kept unchanged, once selected. The typical parameters of the beam are: density $n_b = 0.03n_e$, velocity $V = 3v_T$, where n_e is electron density in the plasma and v_T is the equilibrium thermal velocity of electrons. The beam leads to steady input of energy and heating of the system. Electrons heat up more quickly than ions, therefore two-temperature plasma arises at the initial stage of beam excitation.

The superthermal excitation of plasma oscillations can be detected by comparing dynamical structure factors (DSF) of the plasma under consideration [8,10] for different **k**-vectors with the ones characterizing equilibrium case. The oscillations show up as enhanced and shifted peaks of the DSF.

At the initial stage of plasma excitation by beam the temperature of the electronic component grows too rapidly to allow direct measurement of DSF in MD experiment, which requires averaging over relatively long period of time without significant change of the system characteristics. To overcome this difficulty, the idea of energy exchange with external reservoir is applied to withdraw the energy from the system and keep the average electronic temperature constant for the time of DSF measurement. At first the beam-excited system is allowed to propagate

until its temperature reaches some value T_{I}. Then the propagation of the system continues with additionally applied velocity scaling at every time step, not allowing the electronic temperature to exceed T_{I}. This is performed during the time, sufficient to measure DSF. The resulting DSF characterises the level of plasma excitation by the beam reached at the temperature T_{I}.

To check that the scaling procedure does not change the properties of the system we perform energy freezing consequently first at some intermediate temperature T_{III} and then after release of the velocity scaling at temperature T_{II}. We compare the measurements of system characteristics, including velocity distributions and radial correlation functions with the simulation were the system was allowed to propagate directly to $T_{\mathrm{I}} = T_{\mathrm{II}}$ without intermediate freezing. The time evolution of the component temperatures of the system during this test simulation is shown in the figure 11. The check does not show any significant differences between two measurements.

An example of DSFs measured at temperatures $T_{m1} = 1.2T_0 = 36{,}000\mathrm{K}$ and $T_{m2} = 1.8T_0 = 54{,}000\mathrm{K}$ is shown in figure 12(a)–(c) compared with the equilibrium DSF for different **k**-vectors. As expected, in the case of beam excitation the DSFs show remarkable change of intensity in the peak regions.

8. Multi-scale approaches

Relaxation process can be too long to be simulated by MD in particular for multi-scale systems. In this case a simplified model of the system can be used to increase simulation speed. The results of this model are to be scaled with the help of analytic expressions. Two examples are briefly given below.

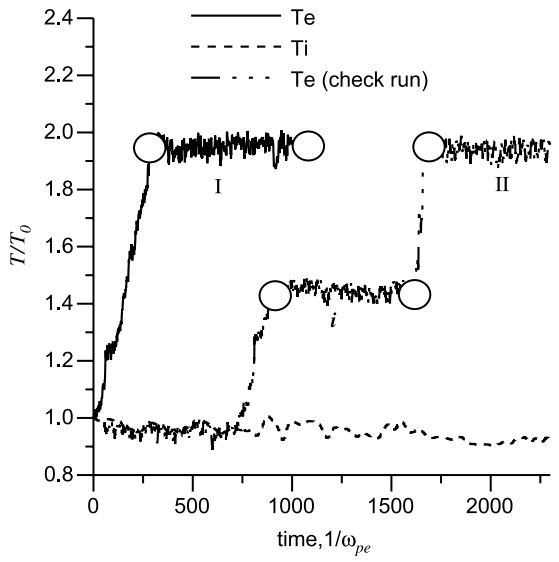

Figure 11. Checking the influence of velocity scaling procedure: the DSF measured for the system in state II (which was subject to scaling procedure at state i with intermediate temperature) is the same as for the system in state I.

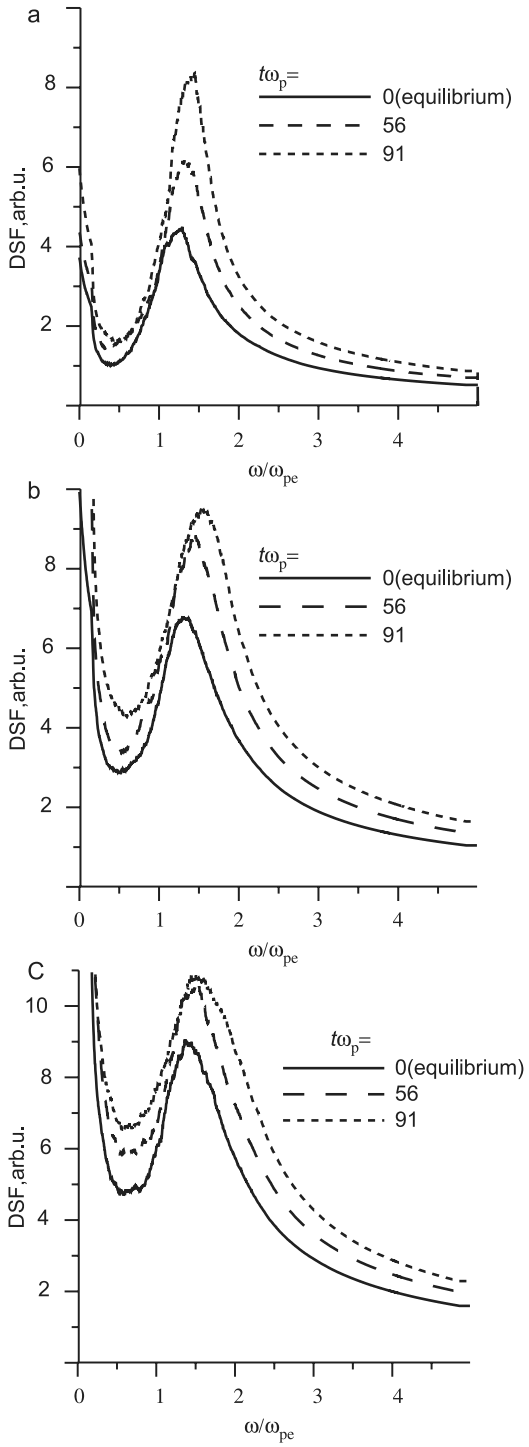

Figure 12. Dynamical structure factors for different stages of plasma excitation drawn for three **k**-vectors starting from minimal allowed in the MD cell. (a) $\mathbf{k} = 0.34R_D^{-1} = 0.78 \times 10^{-10}$ m; (b) $\boldsymbol{k} = 0.49R_D^{-1} = 1.1 \times 10^{-10}$ m; (c) $\boldsymbol{k} = 0.59R_D^{-1} = 1.4 \times 10^{-10}$ m, where R_D is Debye length in equilibrium. The same arbitrary units are used for (a)–(c). Initial conditions: $T_0 = 30{,}000\mathrm{K}$, $\Gamma_0 = 1$. Beam parameters: $n_{\mathrm{b}}/n_{\mathrm{e}} = 0.03$, $v_{\mathrm{b}}/v_T = 3$.

8.1 Dependence of the exponential relaxation time on plasma properties

Unlike the non-exponential relaxation stage in non-ideal plasma the exponential one can be directly compared with

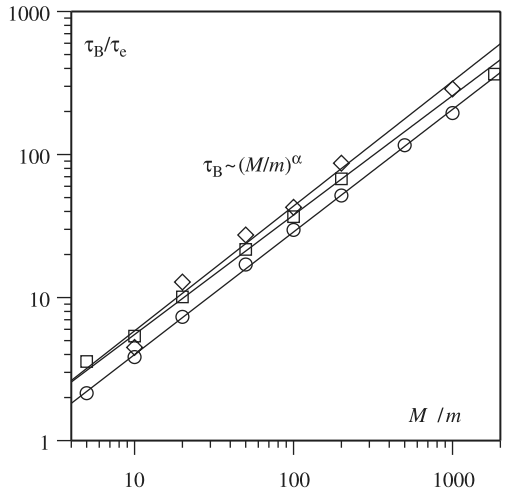

Figure 13. The dependence of the exponential relaxation times on the mass ratio for different initial conditions: $T_i(0) = 0$ (quasi-random)—squares, $T_i(0) = 0$ (crystal)—circles, $T_e(0) = 0$—rhombus. Strait lines correspond to the power fits $\tau_B \sim (M/m)^\alpha$. $\Gamma = 1.28$.

known analytical results for an ideal plasma. The dependence of characteristic relaxation time τ_B on the mass ratio is shown in figure 13. As seen, different initial conditions result in close values of $\tau_B(M)$. Lower relaxation time for the crystal-like initial configuration of ions is caused by an additional heating of ions due to reconfiguration and correlation build up in the ionic subsystem. The mass dependence can be fitted by the power fit $\tau_B/\tau_e \sim (M/m)^\alpha$ in all cases in figure 13. The dependence of α on the non-ideality parameter can be fitted by the parabolic curve

$$\alpha(\Gamma) = 1 - 0.15\,\Gamma + 0.035\,\Gamma^2, \quad 0 < \Gamma < 4. \qquad (1)$$

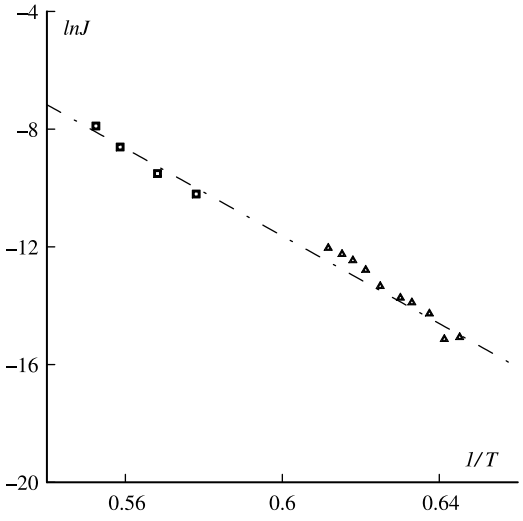

Figure 14. Results of MD calculation of homogeneous nucleation rate in the superheated crystal (Lennard–Jones system, density $N/V = 1.0\sigma^{-3}$): symbols are the values of the homogeneous nucleation rate $J = (V\bar{\tau})^{-1}$ calculated for different temperatures T and system sizes N: squares—$N = 500$, triangles—$N = 6912$. V is the volume of the simulation cell. Dashed line is the best fit using equation (4): $\ln J = -8.9 \times 10^3/T + 42.3$.

The dependencies of τ_B on the ion mass and Γ can be separated as follows

$$\tau_B(\Gamma, M) = \tau_B^1(\Gamma)\left(\frac{M}{m}\right)^{\alpha(\Gamma)}. \qquad (2)$$

The result for $\tau_B^1(\Gamma)$ is presented in [11]. As seen the initial conditions do not affect τ_B^1 significantly. In the weak non-ideality region the MD results are in a good agreement with the Landau theory [43]

$$\tau_B^* = \frac{3}{16}\frac{(mT_i + MT_e)}{\sqrt{2\pi mM}}\frac{1}{e^4 n_e L_e}, \qquad (3)$$

where L_e is the Landau logarithm. For the ideal plasma equation (3) gives $\alpha = 1$ while MD simulations of the non-ideal plasma show that α is usually smaller than unity.

One can estimate the relaxation times in real experimental conditions using given Γ-dependence and mass-dependence. The error of determination of $\alpha(\Gamma)$ is about $\xi_\alpha = 5\%$. The corresponding error of the extrapolation of relaxation times, e.g. for aluminium is $\xi_\tau = \log(M_r/M)\xi_\alpha = 40\%$, where M_r/M is the ratio between real and model ion masses. The obtained precision is enough for comparison by an order of magnitude.

8.2 Nucleation

The value of the average lifetime $\bar{\tau} = \sum_{j=1}^{M} \tau_j/M$ of the metastable state for a given degree of metastability allow one to obtain the homogeneous nucleation rate [19]. The dependence of the homogeneous nucleation rate on temperature following the classical nucleation theory (CNT) has the form

$$J(T) = J_0 \exp\left(\frac{-W}{k_B T}\right), \qquad (4)$$

where k_B is the Bolzmann constant, W is the energy barrier for nucleation. The MD results for the nucleation rate at various temperatures can be fitted by this formula to obtain W and J_0 in the certain temperature range (e.g. figure 14). Then these estimates can be included in the meso- or macroscopic simulation on larger length- and timescales that can not be directly achieved in MD simulation (e.g. [44]).

9. Conclusions

At attempt is done to formulate standard requirements to MD modelling and simulation of relaxation processes in dense media, which would be more or less universal and independent of the physical systems studied. The main features are considered which are new with respect to the simulations of equilibrium systems:

- averaging over MD relaxation runs started from an ensemble of initial non-equilibrium states which correspond to the physical problem under study;
- separate consideration of the initial ensemble-dependent stage of relaxation and subsequent stage which might be ensemble-independent and remind of Boltzmann exponential relaxation;

- calculation of dynamical memory time t_m and comparison of t_m with the duration of the ensemble-dependent stage of relaxation;
- instantaneous and time-averaged measurement procedures which are specific for studying of relaxation processes;
- analytical extrapolation approaches to estimate relaxation times which are too long to be simulated by MD, especially for multi-scale systems.

Three examples of relaxation are considered: equilibration of electrons and ions in non-ideal plasmas, decay of metastable crystals under superheating or stretching. Non-exponential relaxation is observed for different initial conditions and its transition to the exponential regime is confirmed for plasma; dynamic and stochastic stages of the relaxation are shown. Deviation from Maxwellian distribution is observed for different relaxation processes. Nucleation and void formation are simulated.

Acknowledgements

This research is partially supported by grants RFBR 03-11-90272v and NWO 047.016.007/RFBR 04-01-89006 and by Programs of Russian Academy of Sciences 'Parallel computations and multiprocessor computer systems' and 'Information-computer models of study of non-equilibrium media fundamental problems'. AYuK, and VVS are grateful for the support to 'Dynastia' foundation and the International center of fundamental physics in Moscow IVM acknowledges Russian Science Support Foundation. The computations were performed in the computer cluster system granted by Deutscher Akademischer Austauschdienst.

References

[1] M.P. Allen, D.J. Tildesley. *Computer Simulation of Liquids*, Clarendon, Oxford (1987).
[2] W.G. Hoover. *Computational Statistical Mechanics*, Elsevier, Amsterdam (1991).
[3] D.C. Rapaport. *The Art of Molecular Dynamics Simulations*, Cambridge University Press, Cambridge (1995).
[4] D. Frenkel, B. Smit. *Understanding Molecular Simulations*, Academic Press, London (1996).
[5] R. Esser, P. Grassberger, J. Grotendorst, M. Lewerenz (Eds.). *Molecular Dynamics on Parallel Computers*, World Scientific, Singapore (2000).
[6] R.J. Sadus. Molecular simulation of fluids. *Theory, Algorithms and Object-Orientation*, Elsevier, Amsterdam (2002).
[7] J.P. Hansen, I.R. McDonald. Thermal relaxation in a strongly coupled two-temperature plasma. *Phys. Lett. A*, **97**, 42 (1983).
[8] G.E. Norman, A.A. Valuev, I.A. Valuev. Non-equilibrium effects in electron–ion strongly coupled plasmas. Molecular dynamics simulation. *J. Phys. (France)*, **10**(Pr5), 255 (2000).
[9] I.V. Morozov, G.E. Norman. Non-Exponential dynamic relaxation in strongly non-equilibrium non-ideal plasmas. *J. Phys. A: Math. Gen.*, **36**, 6005 (2003).
[10] I.V. Morozov, G.E. Norman, A.A. Valuev, I.A. Valuev. Non-ideal plasma as non-equilibrium media. *J. Phys. A: Math. Gen.*, **36**, 8723 (2003).
[11] I.V. Morozov, G.E. Norman. Collisions and plasma waves in non-ideal plasmas. *J. Exp. Theor. Physics*, in press **100** (2005).
[12] G. Zwicknagel. Molecular dynamics simulations of the dynamics of correlation and relaxation in OCP. *Contrib. Plasma Phys.*, **39**, 155 (1999).
[13] S.G. Kuzmin, T.M. O'Neil. Numerical simulation of ultracold plasmas: how rapid intrinsic heating limits the development of correlation. *Phys. Rev. Lett.*, **88**, 65003 (2002).
[14] S.G. Kuzmin, T.M. O'Neil. Numerical simulation of ultracold plasmas. *Phys. Plasmas*, **9**, 3743 (2002).
[15] S. Mazevet, L.A. Collins, J.D. Kress. Evolution of ultracold neutral plasmas. *Phys. Plasmas*, **88**, 055001 (2002).
[16] T. Nguyen, P.S. Ho, T. Kwok, C. Nitta, S. Yip. Thermal structural disorder and melting at a crystalline interface. *Phys. Rev. B*, **46**, 6050 (1992).
[17] G.E. Norman, V.V. Stegailov. Homogeneous nucleation in a superheated crystal. Molecular dynamics simulation. *Dokl. Phys.*, **47**, 667 (2002).
[18] G.E. Norman, V.V. Stegailov, A.A. Valuev. Nanosecond electric explosion of wires: from solid superheating to non-ideal plasma formation. *Contrib. Plasma Phys.*, **43**, 384 (2003).
[19] G.E. Norman, V.V. Stegailov. Simulation of ideal crystal superheating and decay. *Mol. Simul.*, **30**, 397 (2004).
[20] A.Y. Kuksin, G.E. Norman, V.V. Stegailov. Simulation of ideal crystal superheating and decay. *Proceedings Joint Conference of ICCP6 and CCP2003*, Rinton Press, Princeton, NJ (2004).
[21] D.A. Firsov, B.L. Grigorenko, A.V. Nemukhin, L.Y. Khriachtchev, M.O. Rasanen. Emission of SH radicals in solid krypton: mixed quantum-classical molecular dynamics simulations. *Chem. Phys. Lett.*, **338**, 317 (2001).
[22] C.D. Snow, H. Nguyen, V.S. Pande, M. Gruebele. Absolute comparison of simulated and experimental protein-folding dynamics. *Nature*, **420**, 102 (2002).
[23] V.Y. Klimenko, A.N. Dremin. Structure of the shock wave front in solid. *Dokl. AN USSR*, **251**, 1379 (1980).
[24] V.Y. Klimenko, A.N. Dremin, *et al.* Structure of the shock wave front in solid. In *Progress in Astronautics and Aeronautics*, J. Belak (Ed.), vol. 75, pp. 253–268, AIAA Inc., Washington, DC (1981).
[25] V.V. Zhakhovskii, S.V. Zybin, K. Nishihara, S.I. Anisimov. Orientation dependence of shock structure with melting in L-J crystal from molecular dynamics. *Prog. Theor. Phys. Suppl.*, **138**, 223 (2000).
[26] D. Tanguy, M. Mareschal, P.S. Lomdahl, T.C. Germann, B.L. Holian, R. Ravelo. Dislocation nucleation induced by a shock wave in a perfect crystal: Molecular dynamics simulations and elastic calculations. *Phys. Rev. B*, **68**, 144111 (2003).
[27] L. Stella, S. Melchionna. Equilibration and sampling in molecular dynamics simulations of biomolecules. *J. Chem. Phys.*, **109**, 10115 (1998).
[28] B. Heymann, H. Grubmüller. Molecular dynamics force probe simulations of antibody/antigen unbinding: Entropic control and non-additivity of unbinding forces. *Biophys. J.*, **81**, 1295 (2001).
[29] A.A. Darinskii, A. Zarembo, N.K. Balabaev, I.M. Neelov, F. Sundholm. Molecular dynamics simulation of a flexible polymer network in a liquid crystal solvent; structure and equilibrium properties. *Polymer*, **45**, 4857 (2004).
[30] M.A. Mazo, M.Y. Shamaev, N.K. Balabaev, A.A. Darinskii, I.M. Neelov. Conformational mobility of carbosilane dendrimer: Molecular dynamics simulation. *Phys. Chem. Chem. Phys.*, **6**, 1285 (2004).
[31] A.L. Rabinovich, P.O. Ripatti, N.K. Balabaev, F.A.M. Leermakers. Molecular dynamics simulations of hydrated unsaturated lipid bilayers in the liquid-crystal phase and comparison to self-consistent field modeling. *Phys. Rev. E*, **67**, 011909 (2003).
[32] V.L. Golo, K.V. Shaitan. Dynamic attractor associated with the Berendsen thermostat and slow dynamics of biological macromolecules. *Biophysics*, **47**, 611 (2002).
[33] V.Y. Rudyak, G.V. Kharlamov, A.A. Belkin. Diffusion of nanoparticles and macromolecules in dense gases and liquids. *High Temp.*, **39**, 283 (2001).
[34] I.V. Morozov, G.E. Norman, A. Valuev. Stochastic properties of strongly coupled plasmas. *Phys. Rev. E*, **63**, 36405 (2001).
[35] G.E. Norman, V.V. Stegailov. The stochastic properties of a molecular-dynamical Lennard–Jones system in equilibrium and non-equilibrium states. *J. Exp. Theor. Phys.*, **92**, 879 (2001).
[36] G.E. Norman, V.V. Stegailov. Stochastic and dynamic properties of molecular dynamics systems: Simple liquids, plasma and electrolytes, polymers. *Comput. Phys. Comm.*, **147**, 678 (2002).
[37] V.Y. Rudyak, G.V. Kharlamov. The theory of equilibrium fluctuations of thermodynamic quantities in open systems with a small number of particles. *High Temp.*, **41**, 237 (2003).
[38] D.O. Gericke, M.S. Murillo, D. Semkat, M. Bonitz, D. Kremp. Relaxation of strongly coupled Coulomb systems after rapid

changes of the interaction potential. *J. Phys. A: Math. Gen.*, **36**, 6087 (2003).

[39] W. Ebeling, G.E. Norman, A.A. Valuev, I.A. Valuev. Quasiclassical theory and molecular dynamics of two-component non-ideal plasmas. *Contrib. Plasma Phys.*, **39**, 61 (1999).

[40] G. Kanel, S. Razorenov, K. Baumung, J. Singer. Dynamic yield and tensile strength of aluminum single crystals at temperatures up to the melting point. *J. Appl. Phys.*, **90**, 136 (2001).

[41] S.-N. Luo, T.J. Ahrens, T. Çağin, A. Strachan, W.A.G. Goddard III, D.C. Swift. Maximum superheating and undercooling: systematics, molecular dynamics simulations, and dynamic experiments. *Phys. Rev. B.*, **68**, 134206 (2003).

[42] P. Gibbon, S. Pfalzner. Direct calculation of inverse-Bremsstrahlung absorption in strongly coupled, non-linearly driven laser plasmas. *Phys. Rev. E*, **57**, 4698 (1998).

[43] E.M. Lifshitz, L.P. Pitaevskii. *Physical Kinetics*, Pergamon, Oxford (1981).

[44] S.P. Zhvavy. Simulation of the melting and crystallization processes in monocrystalline silicon exposed to nanosecond laser radiation. *Tech. Phys.*, **45**, 1014 (2000).